Radial deformation-induced high-capacity hydrogen storage in Li-coated zigzag boron nanotubes

Hui An, Chun-Sheng Liu,* and Zhi Zeng†

Key Laboratory of Materials Physics, Institute of Solid State Physics, Chinese Academy of Sciences, Hefei 230031, People's Republic of China and Graduate School of the Chinese Academy of Sciences, Beijing 100094, People's Republic of China

(Received 29 September 2010; revised manuscript received 29 January 2011; published 29 March 2011)

We show that a Li-coated zigzag (2,2) boron nanotube can serve as a high-capacity hydrogen storage medium using first-principles density functional theory. The present results indicate that the radial deformation of a Li-coated boron nanotube can strengthen the binding of Li atoms to the boron nanotube due to the hybridization between Li-*p* orbitals and B-*p* orbitals. Interestingly, the induced large surface curvature of the Li-coated nanotube can make the H_2 molecules directly adsorbed on the nanotube. Through the electronic analysis we find that not only the polarization mechanism but also the orbital hybridization between H-*s* orbitals and Li-*p* (B-*p*) orbitals act on the adsorbed H_2 molecules. The Li-coated zigzag (2,2) boron nanotube reported here can store hydrogen up to 7.94 wt% with the adsorption energy of 0.12–0.20 eV/H_2 and the whole system is favorable for the reversible hydrogen adsorption/desorption at ambient conditions.

DOI: 10.1103/PhysRevB.83.115456 PACS number(s): 68.43.Bc, 31.15.A−, 61.46.Fg, 84.60.Ve

I. INTRODUCTION

Hydrogen is being considered as an important element for future energy schemes because of its efficiency, abundance, and environmental friendliness.[1] However, one of the most difficult challenges in realizing hydrogen economy is to find materials that can store hydrogen with high gravimetric and volumetric density at near ambient thermodynamic conditions.

In recent years, carbon-based nanostructures have widely attracted attention as potential hydrogen storage media, for example, carbon nanotubes (CNT),[2,3] carbon fullerenes,[4–8] ethylenes,[9–11] and graphenes.[12–15] However, H_2 molecules bind weakly to pristine carbon materials via van der Waals interactions. Therefore, coating the carbon surfaces with metal atoms has recently been presented to improve storage performance. On the one hand, coating carbon nanostructures with early transition-metals (TM)[2,6,9] can enhance the hydrogen adsorption energies up to 0.2–0.6 eV/H_2 via the Kubas interaction.[16,17] Unfortunately, homogeneously coating carbon surfaces with TM atoms are metastable and the TM atoms would cluster on the surfaces.[4] In addition, the dissociation of the first H_2 molecule added to the TM atoms will also lower the gravimetric density. On the other hand, it was suggested that alkali metals (AM) and alkaline-earth metals (AEM), especially Li (Ref. 3) and Ca (Refs. 7 and 13), can produce a uniform coating due to their lightweight and lower cohesive energies (1.5–2 eV) than those of TM (∼4 eV). Besides the uniform distribution of metal atoms, the adsorption energy of H_2 molecules should lie between the physisorbed and the chemisorbed states. Early studies claimed that the storage materials should bind the H_2 molecules with the adsorption energy of 0.2–0.6 eV/H_2 (Refs. 18 and 19) or 0.2–0.7 eV/H_2 (Ref. 3) whereas some other studies have proposed that the optimal adsorption energy for mobile applications under room temperature and moderate pressure should be in the range of 0.1–0.2 eV/H_2 (Ref. 20). Recently, some Li- and Ca-coated materials have shown excellent achievements with the desirable adsorption energy.[14,21–23]

Nowadays some groups turn their attention to some novel boron-based nanostructures, such as planar sheet,[24] fullerenes,[25] and single-walled nanotubes,[26–28] which possess the same merits as the C-based materials: lightweight and porous. AM-coated planar boron sheet[29] and B_{80} fullerenes,[22] and Ca-coated B_{80} fullerenes (boron nanaotube)[23] were reported as reversible storage materials due to their strong binding with metal aotms [e.g., the Li-coated planar boron sheet can possess a binding energy of 1.80 eV/atom, which is much higher than the cohesive energy of Li (Ref. 30)]. In addition, the B-doped carbon materials also achieved better results. For example, the B-doped graphene can adsorb the Li atoms with the binding energy of 3.47 eV/atom whereas the pristine graphene merely attaches the Li atoms with the binding energy of 1.14 eV/atom.[14] All these results indicate that the B-contained materials can be considered as promising reversible host materials for hydrogen storage.

In this work, we choose boron nanotubes (BNTs) as the host materials, which might also have the potential to assemble reversible hydrogen storage materials with the lightweight Li atoms. Our main concerns are listed as follows. (i) Can the strength of the bonding between Li and BNT be strong enough to hinder the clustering of Li atoms? What is the mechanism of the bonding? (ii) Is there an evident radial deformation of nanotubes as the number of attached Li atoms increases? How does the radial deformation affect the adsorption of H_2 molecules? (iii) What is the nature of the bonding of H_2 molecules to Li-coated BNT?

II. COMPUTATIONAL DETAILS

Our first-principles calculations are based on spin-polarized density functional theory at the level of generalized gradient approximation (GGA)[31,32] using the Perdew-Wang (1991) functional[33] as implemented in DMOL^3 package. The all-electron (AE) core treatment and a double numerical basis with polarization (DNP) set are adopted. All the obtained structures are optimized without any symmetry constraints. In the self-consistent-field calculations, the electronic-density convergence is set to 1×10^{-6} e/Å^3. The convergence criteria during geometry optimization are 10^{-5} Hartree for the energy, 2×10^{-3} Hartree/Å for the force, and 5×10^{-3} Å for atomic

displacements. The k point is set to $1 \times 1 \times 3$ and the global cutoff radius is 5.1 Å for all calculations.

Here we will follow the same vectors that were introduced by Ni *et al.*[27] to determine the BNT. The (2,2) BNT is set as the host material. The calculations are carried out in a cubic supercell geometry of 25 Å × 25 Å × c, where the c equals twice the periodicity of the nanotube.

III. RESULTS AND DISCUSSIONS

A. Coating BNT with a single Li atom and its mobility and stability

We first investigate the deposition of a single Li atom on the BNT (BNT-Li complex). After varying the position of the Li atom and relaxing all structures, we find that the optimal position of Li turns out to be above the center of the empty boron hexagon, as shown in Fig. 1(a). To check the stability of our model, the binding energy (E_b) between Li and the nanotube is defined as

$$E_b = (1/n)[E(BNT) + nE(Li) - E(BNT - nLi)], \quad (1)$$

where E(BNT), E(Li), and E(BNT-nLi) are the energy of the pristine BNT, the energy of a free Li atom, and the total energy of the BNT with n adsorbed Li atoms, respectively.

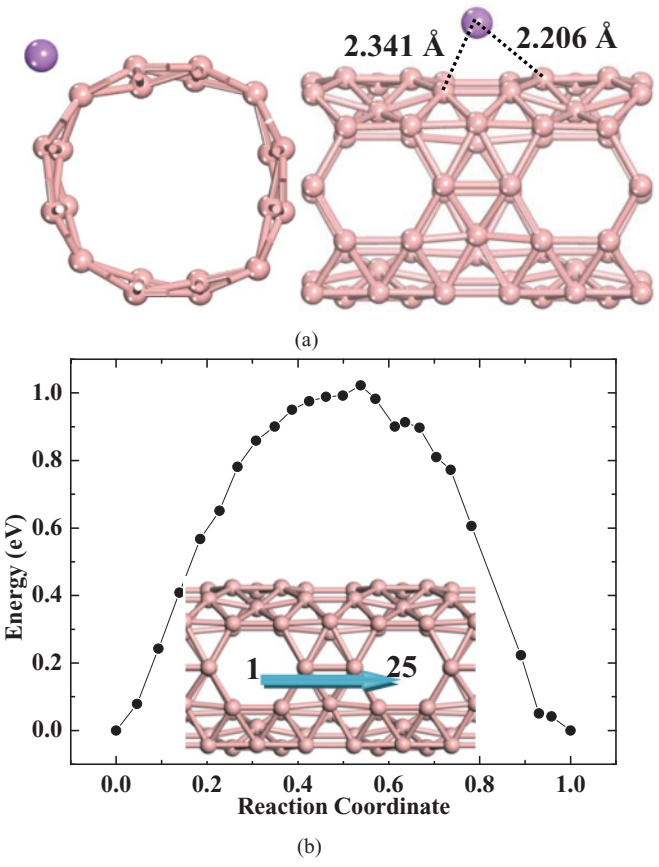

FIG. 1. (Color online) (a) Top view and side view of the optimized structure of a (2,2) BNT coated with a single Li atom. Here the large and small balls represent the Li and B, respectively. (b) The calculated energy plots for the diffusion of a Li atom over the BNT surface using the NEB calculations. We choose 25 images along the minimum-energy path. The calculated energy barrier is 1.02 eV.

The calculated value of E_b = 1.92 eV is larger than the formation heat for the Li atom in the gas phase of 1.62 eV (Ref. 30). It is known that the stability of a material such as a Li-coated BNT depends on the mobility of the metal atoms on its surface because the diffusion of a single metal atom always serves as the first step in a clustering process. We then calculate the energy barrier as one Li atom diffuses from the hexagonal site to a neighboring one using the nudged elastic band (NEB) method.[34–36] As shown in Fig. 1(b), the obtained high energy barrier of 1.02 eV makes one individual Li atom thermodynamically stable above the empty hexagonal.

B. Coating BNT with multiple Li atoms and the binding mechanism

To achieve a higher capacity of storing H_2 molecules, now we turn to discuss the structure and properties of eight Li atoms coated BNT (BNT-8Li complex), where Li atoms occupy above all the empty boron hexagons. Interestingly, we find that the tube is deformed into a quadrangular one [Fig. 2(a)], but the Li-Li distance is still more than 5 Å which makes each Li atom adsorb the H_2 molecules independently. Because previous studies have revealed that metal atoms attached on some host materials are easy to cluster as the number of metal atoms increases, one may wonder whether the attached Li atoms reported here would like to remain isolated or aggregate together. As shown in Figs. 3(c) and 3(d), the configuration that Li atoms form a cluster is 4.34 eV higher in energy than when they remain isolated, indicating that the coating complex is rather stable. To further test the stability of the isolated BNT-8Li complex, we perform the finite-temperature *ab initio* molecular-dynamics (MD) simulations on this complex at 300 K with a time step of 1 fs. After running 5000 steps, the geometry is still kept and we do not observe any tendency toward clustering of Li atoms.

The calculated average binding energy per Li atom on BNT is 2.45 eV/atom, which is larger than that in the BNT-Li complex, namely 1.92 eV. However, it has been found that the average binding energy per Li atom on other host materials decreases slightly with the number of adsorbed Li atoms increasing.[3] An explanation of this remarkable difference of the binding energy is sought in the electronic energy structure and partial density of states (PDOS). Figure 2(b) illustrates the PDOS of the BNT-8Li complex, where Li p orbitals participate in the bonding. The attached Li first donates the s electrons to

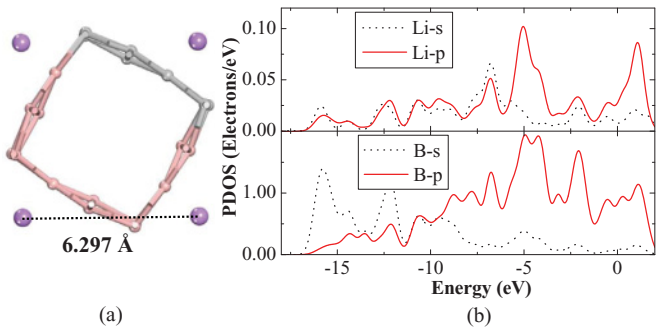

FIG. 2. (Color online) (a) Top view of the optimized configuration of a (2,2) BNT coated with 8 Li atoms. (b) The partial density of states (PDOS) of Li and B atoms in BNT-8Li complex.

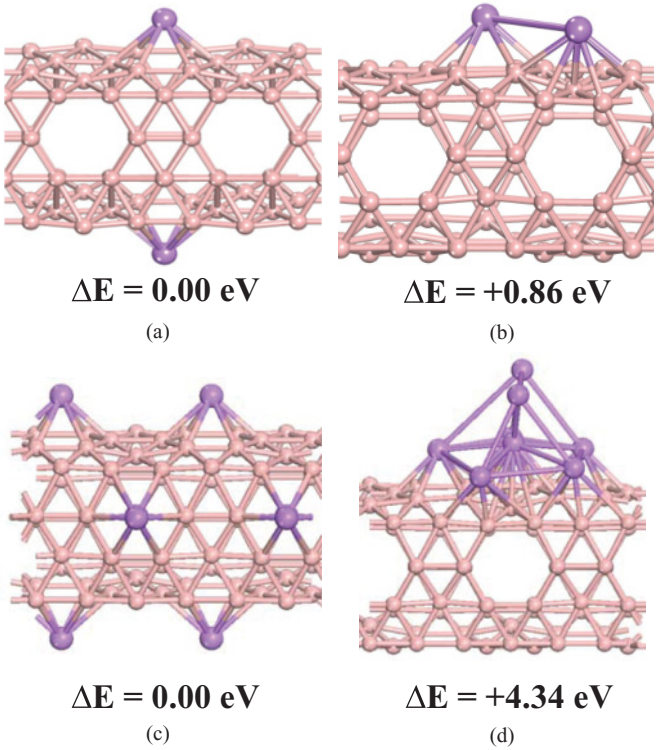

FIG. 3. (Color online) (a) Isolated and (b) dimeric configurations of the BNT-2Li complex. The relative energy ΔE represents the total energy discrepancy between these two different configurations, which is evaluated referring to the isolated one. (c) Isolated and (d) clustered configurations of the BNT-8Li complex. The ΔE is also evaluated referring to the isolated one.

the BNT so that B *p* orbitals are partially filled. Meanwhile, the empty *p* orbitals of the Li will split under the strong ligand field generated by the BNT. Then the BNT back donates some electrons to the low-lying Li *p* orbitals, leading to a strong hybridization between B 2*p* and Li 2*p* orbitals. This bonding mechanism can also be observed in the case of Li binding onto B_{80} fullerenes[22] and boron-doped graphenes.[14] An obvious radial deformation of BNT has been observed as the amount of attached Li atoms increases, which will affect the ligand field, and thus affect the amount of electrons back denoted from BNT to Li empty *p* orbitals. The Mulliken charge analysis (Table III) clearly shows that the Li of BNT-Li complex denotes more *s* electrons to the B substrate than that in the BNT-8Li complex, whereas the B substrate of BNT-8Li complex back donates more electrons to the Li empty *p* orbitals than that in the BNT-Li complex. The *p*-*p* hybridization is substantially stronger than the *s*-*p* hybridization, so the average binding energy per Li atom on BNT in the BNT-8Li complex possesses a higher value but with a relatively smaller net charge transfer. The increase of binding energy per Li atom on BNT is more effective to prevent the clustering of Li atoms, which is helpful to the reversibility.

C. Hydrogen adsorption on BNT-Li complex

To inspect the interaction of H_2 molecules with Li-coated BNT, we define the hydrogen adsorption energy (E_{ad}) as,

$$E_{ad} = E[BNT - mLi - (n-1)H_2] + E(H_2) - E(BNT - mLi - nH_2), \quad (2)$$

and the average hydrogen adsorption energy (E_{aad}) as,

$$E_{aad} = (1/n)[E(BNT - mLi) + nE(H_2) - E(BNT - mLi - nH_2)], \quad (3)$$

where the E(BNT-mLi-$n$$H_2$) is the total energy of BNT-mLi complex with n adsorbed H_2 molecules. The "m" and "n" indicate the numbers of Li atoms and H_2 molecules. We begin with the results of H_2 molecules adsorbed on BNT-Li complex. The first H_2 molecules is adsorbed in molecular form, which prefers to be parallel to the surface of the BNT as highlighted in Fig. 4 with a large binding energy of 0.21 eV. Step by step, we add additional H_2 molecules close to the Li atom of BNT-Li complex. The average adsorption energies (E_{aad}) of H_2 molecules are in the optimal range of 0.14–0.21 eV/H_2 (Table I), which are as large as that found in the case of Ca coated on a (3,3) BNT adsorbing the H_2 molecules.[23] In particular, the average adsorption energy (E_{aad}) of the BNT-Li-4H_2 system can reach up to 0.14 eV/H_2, however, the corresponding adsorption energy (E_{ad} = 0.05 eV) seems too small. Hence the fourth H_2 molecule attached to Li is not thermodynamically stable at room temperature.

D. Hydrogen adsorption on BNT-8Li complex and the interaction mechanism

As stated above, the geometry structure of BNT has changed obviously when eight Li atoms are attached to BNT. The tube is

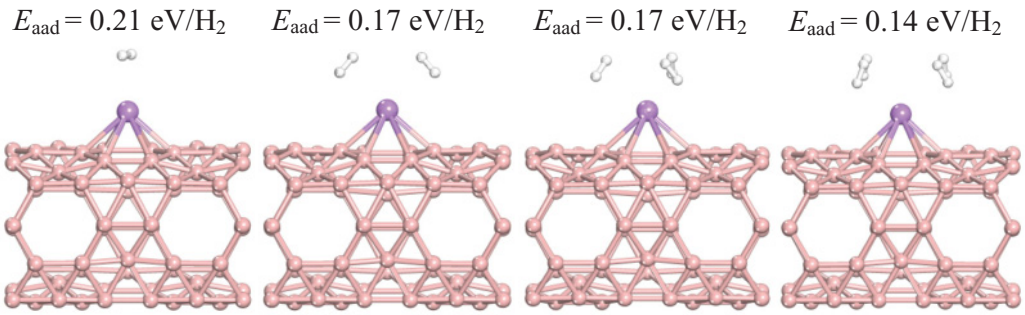

FIG. 4. (Color online) Optimized configurations of Li-coated (2,2) boron nanotube with one to four adsorbed H_2 molecules. Here the large, medium, and small balls represent the Li, B, and H, respectively.

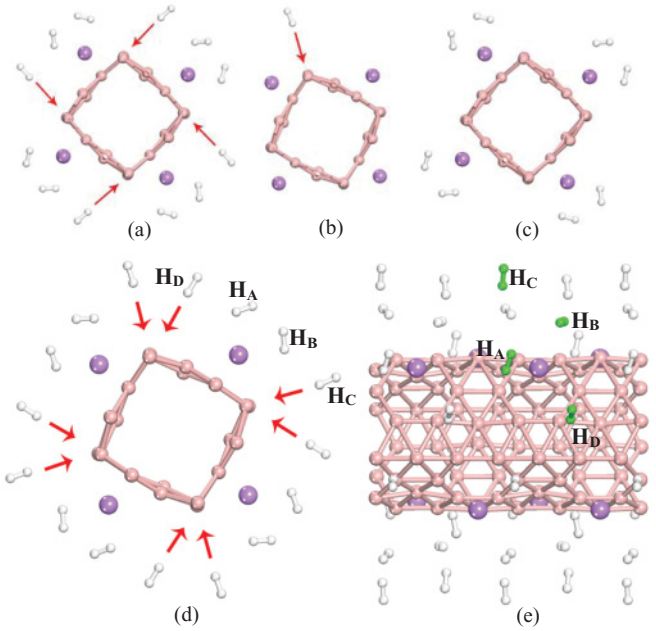

FIG. 5. (Color online) (a) Top view of the BNT-8Li-24H_2 system. The H_2 molecules moving toward the corner are indicated by red arrows. (b) Top view of the optimized configuration of a single H_2 molecule attached to the corner of BNT-8Li complex. The adsorption energy is 0.14 eV. (c) Top view of BNT-8Li-16H_2 system. The first two H_2 molecules are adsorbed by the Li atoms closely. (d) Top view and (e) side view of the optimized configuration of the BNT-8Li-32H_2 system. The different kinds of adsorbed H_2 molecules are indicated as H_A–H_D, respectively.

TABLE I. Average adsorption energies (E_{add}) and adsorption energies (E_{ad}) of H_2 on BNT-Li complex and the corresponding bond lengths.

System	E_{aad} (eV/H_2)	E_{ad} (eV/H_2)	d_{H-H} (Å)	d_{Li-H} (Å)
BNT-Li-H_2	0.21	0.21	0.752	2.097–2.106
BNT-Li-2H_2	0.17	0.14	0.753	2.198–2.300
BNT-Li-3H_2	0.17	0.17	0.752–0.753	2.281–2.399
BNT-Li-4H_2	0.14	0.05	0.751–0.752	2.510–2.704

deformed into a quadrangular one, resulting in a large surface curvature in the corner. One may wonder whether this radial deformation will affect the hydrogen uptaking in the BNT-8Li complex. In detail, when three H_2 molecules are adsorbed around each Li atom of BNT-8Li complex, one H_2 molecule moves to the corner [indicated by red arrows in Fig. 5(a)]. A similar phenomenon can also be observed when multiple Ca atoms bind on a (3,3) BNT.[23] Consequently, we turn to analyze the adsorption of a single H_2 molecule to the corner of BNT-8Li complex, as shown in Fig. 5(b). Surprisingly, the adsorption energy of this H_2 molecule can reach up to 0.14 eV. It is obvious that the corner of BNT is attractive for the H_2 molecules as well as the coated metal atoms. Since there is still much spare room around the corner, it is easy to image adding more H_2 molecules around the corner to increase the hydrogen storage capacity. As shown in Figs. 5(d) and 5(e), eight more H_2 molecules are attached to the corners of the former BNT-8Li-24H_2 system. Seen from Table II, the calculated adsorption energies (E_{ad}) of BNT-8Li-24H_2 and BNT-8Li-32H_2 systems [Figs. 5(a) and

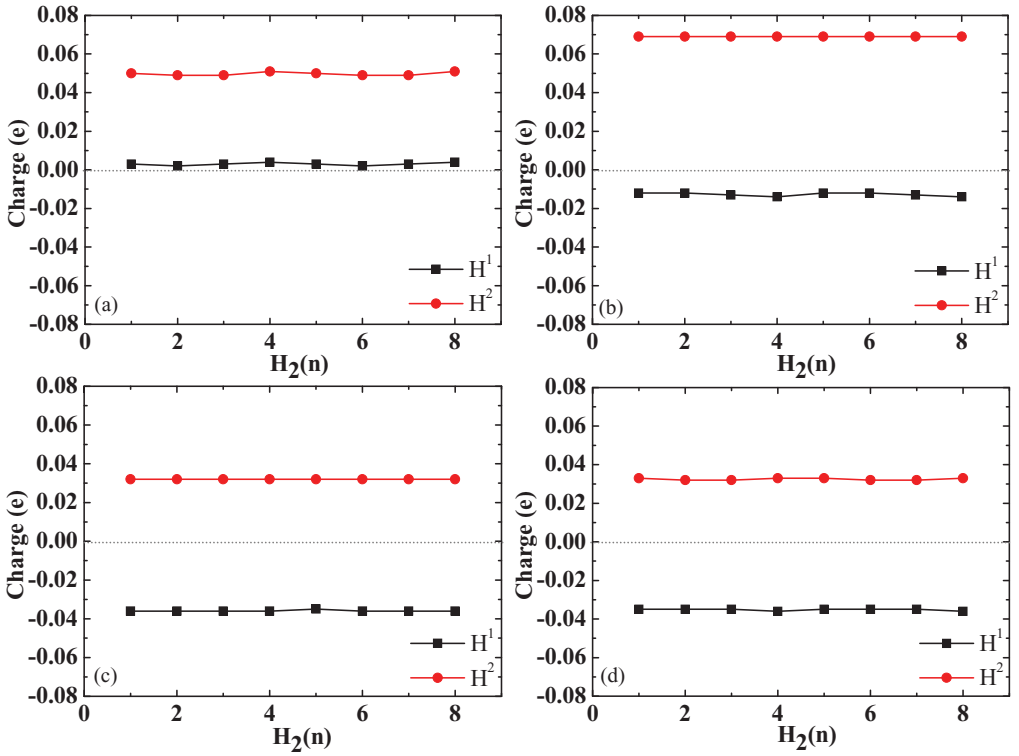

FIG. 6. (Color online) Here H^1 and H^2 represent the charge of two different hydrogen atoms in one H_2 molecule of BNT-8Li-32H_2 system where the H^2 atom is closer to the Li or B atoms than the H^1 one. $H_2(n)$ indicates the H_2 molecules attracted by/close to the different Li atoms coated on BNT. (a–d) show the H^1 and H^2 values of H_A–H_D, respectively.

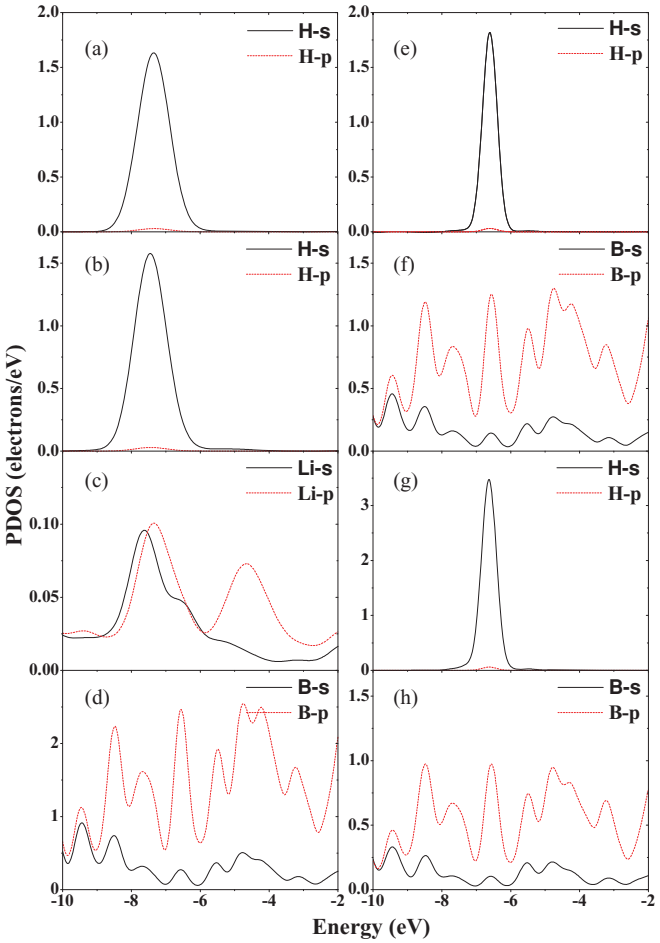

FIG. 7. (Color online) The PDOS under the Fermi level E_F: (a) H_A, (b) H_B, (c) Li, and (d) B atoms close to Li, (e) H_C, (f) B atoms close to H_C, (g) H_D and (h) B atoms close to H_D in the BNT-8Li-32H_2 system.

5(d)] are 0.13 and 0.12 eV/H_2, whereas the corresponding average adsorption energies (E_{aad}) are 0.16 and 0.15 eV/H_2, respectively.

To conveniently discuss the binding mechanism of H_2 molecules on BNT-8Li, we classify hydrogen molecules as two sets as shown in Figs. 5(d) and 5(e): one (indicated as H_A and H_B) is adsorbed around the Li atoms and the other (indicated as H_C and H_D) is located around the corners of BNT. For H_A and H_B, the binding mechanism of H_2 molecules to BNT-8Li complex is in essence the same as that of H_2 molecules on AM-coated B_{80} (Ref. 22) and Li-coated CNT,[3] which is related

TABLE II. The average hydrogen adsorption energies (E_{add}) and hydrogen adsorption energies (E_{ad}) of BNT-8Li complex with different numbers of adsorbed H_2 molecules in Fig. 4.

System	E_{aad} (eV/H_2)	E_{ad} (eV/H_2)	d_{H-H} (Å)
BNT-8Li-8H_2	0.20	0.20	0.754–0.756
BNT-8Li-16H_2	0.17	0.16	0.754–0.756
BNT-8Li-24H_2	0.16	0.13	0.752–0.756
BNT-8Li-32H_2	0.15	0.12	0.752–0.756

TABLE III. The Mulliken atomic charge of Li atoms in BNT-Li complex, BNT-8Li complex and BNT-8Li-32H_2 system.

Li atom	BNT-Li	BNT-8Li	BNT-8Li-32H_2
Net charge (e)	+0.131	+0.067	−0.003–0.001
2s (e)	0.289	0.325	0.345–0.347
2p (e)	0.517	0.542	0.582–0.584

to the high electric field near the AM atoms. As summarized in Table III, the Li atoms partially donate their valence electrons to the B substrate, which binds H_2 in a molecular form due to the polarization mechanism.[37] In addition, with the help of Mulliken charge analysis, it is clearly seen from Figs. 6(a) and 6(b) that the H atoms close to Li atoms lose more electrons than the ones far from Li atoms, which can also be confirmed through the deformation charge distribution [Fig. 8(b)]. Here, the small charge transfer from H_A and H_B to BNT-8Li complex can be explained by an evident hybridization between H s and Li 2p orbitals. As revealed in Figs. 7(a) through 7(d), the peaks of Li p orbitals located at −7.67, −4.74, and −1.82 eV hybridize with H_A and H_B in the lower energy range, where H s orbitals overlap with the Li 2p orbitals at −7.67 eV. On the other hand, the bands of Li also interact with those of B substrate around the energies of −7.70, −4.74, and −1.82 eV, where some sharp peaks of Li 2p orbitals and/or 2s orbitals can be observed. This suggests that Li acts as a "bridge" in this reaction, which interacts with the H_2 molecules and the B substrate simultaneously. This binding has also been observed in the case of H_2 molecules adsorbed on Li-coated CNT.[3] As a result, parts of the charge of H_2 molecules will finally transfer to the B substrate through the Li atoms, this can also be confirmed by Mulliken charge analysis [Figs. 6(a) and 6(b) and Table III] which clearly indicates that H_A and H_B donate totally more than 0.10 e to BNT-8Li complex, whereas the attached Li merely accepts about 0.07 e, so the surplus charge will transfer to the B substrate. It is obvious that the orbital hybridization between H s and Li 2p orbitals is helpful to the adsorption of H_2 molecules (H_A and H_B) on BNT-8Li complex.

Interestingly, the H_2 molecules (H_C and H_D) are adsorbed around the corner of BNT with optimal adsorption energies. On the contrary, the binding of H_2 molecules to the pristine boron nanotubes and carbon nanotubes is very weak. Upon the attachment of eight Li atoms, the surface curvature at the corner becomes very large where the angle formed by two faces is approximately 90°, resulting in a relatively high charge density distribution at the corner [Fig. 8(a)] that makes the corner capable of adsorbing the H_2 molecules strongly. A recent report[38] has claimed that molecular adsorption in pristine carbon-based materials is explicitly dependent upon the curvature of graphitic nanostructures [e.g., the graphite binds the H_2 molecules with very small adsorption energies of 0.04 eV/H_2 (Ref. 38) whereas the $C_{35}B$ cluster with a small radius can bind the H_2 molecules with adsorption energies of 0.39 eV/H_2].[39] In detail, as shown in Figs. 6(c) and 6(d), it is obvious that there is no significant charge transfer existing between the H_2 molecules and BNT-8Li complex ($H^1 \approx -H^2$). Therefore the polarization interactions still mainly contribute

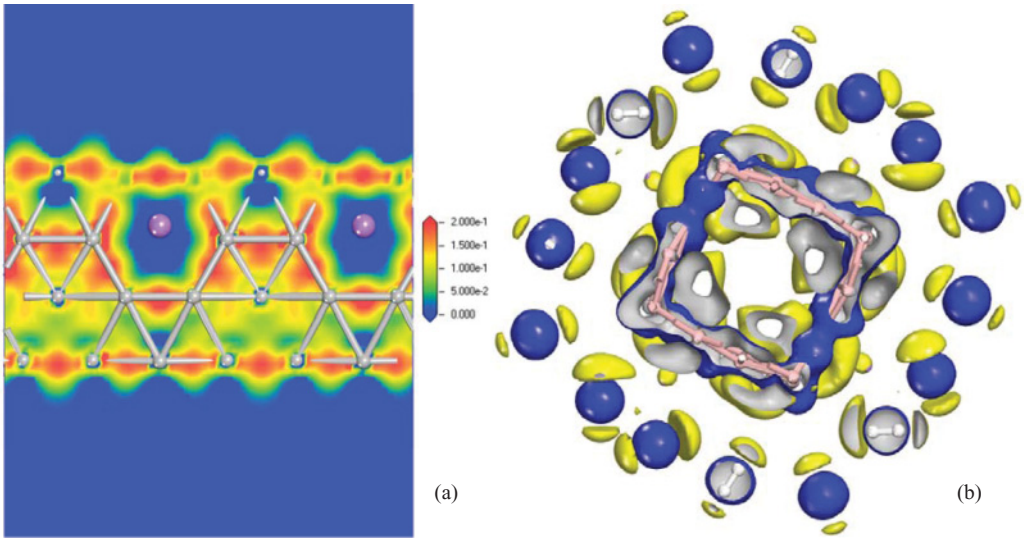

FIG. 8. (Color online) (a) The two-dimensional deformation charge density distribution of the boron surface marked in gray color [Fig. 2(a)]. A color spectra spans from blue to red represent value from 0 to 2.0×10^{-1} e/Å^3. The charge density of the B atoms at the corner is as high as that of the B atoms bound to Li. (b) The deformation charge density distribution of the BNT-8Li-32H_2 system. The deformed density marked in blue corresponds to the region that contains excess electrons, while that marked in yellow indicates electron loss. The isosurface value is about 0.03 e/Å^3.

to the binding of BNT-8Li complex with H_C and H_D, which involves the charge redistribution in the polarized H-H dipoles. As a result, the H-H bond lengths slightly expand from 0.745 Å (the value of the free molecular state) to 0.752–0.754 Å. In addition, seeing from a further comparison of the accurate value of H^1 and H^2, we have found that the absolute value of the former one is slightly larger than that of the latter one (namely, -0.037 *e* for H^1 and 0.032 *e* for H^2), indicating that there exists a very small charge transfer from the B substrate to H_2 molecules. This can also be confirmed by the deformation charge density distribution [Fig. 8(b)] which clearly indicates that the charge around those H atoms is visible. Comparing Figs. 7(e) [7(g)] with Figs. 7(f) [7(h)], it

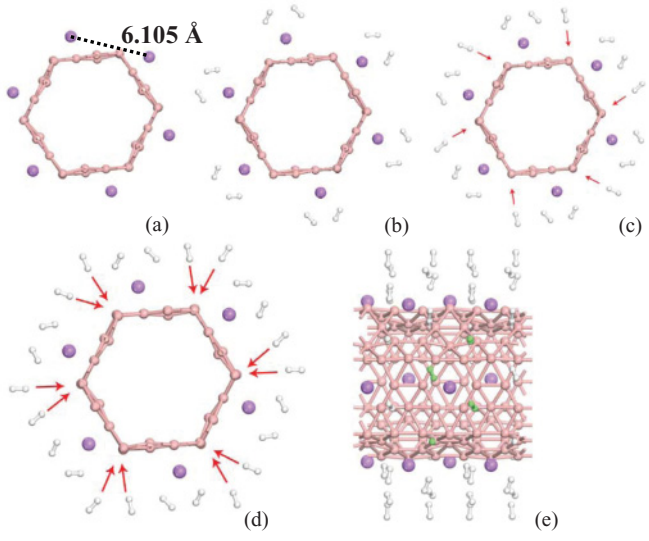

FIG. 9. (Color online) (a) Top view of the multiple Li coated (3,3) BNT, the calculated E_b between the Li atom and the BNT is 2.27 eV. (b) Top view of the $BNT_{(3,3)}$-12Li-24H_2 system. The first two attached H_2 molecules can be adsorbed by each Li atom closely. (c) Top view of the $BNT_{(3,3)}$-12Li-36H_2 system. The H_2 molecules moving toward the corners are indicated by red arrows. (d) Top view and (e) side view of the $BNT_{(3,3)}$-12Li-48H_2 system.

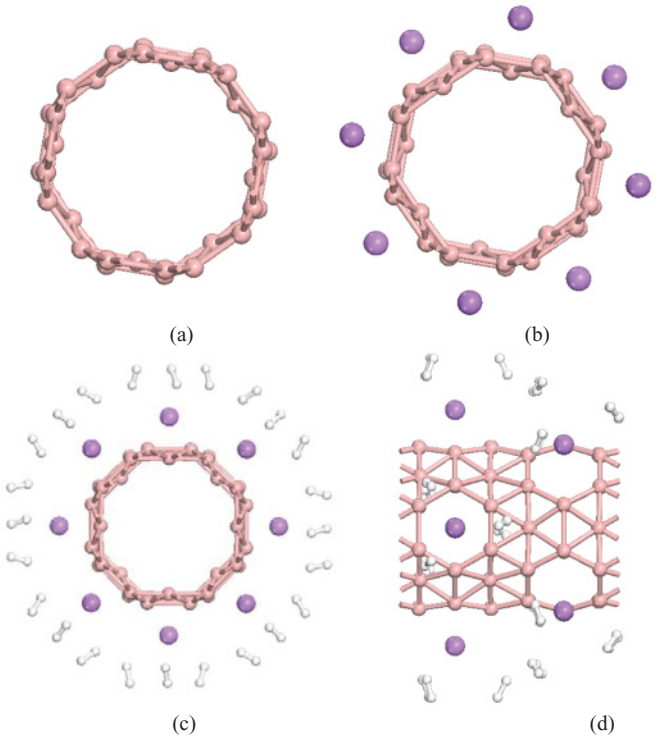

FIG. 10. (Color online) (a) Top view of the (4,0) BNT and (b) top view of the multiple Li-coated (4,0) BNT. The comparison of these two configurations indicates that the nanotube does not change obviously and the calculated E_b of Li onto the BNT is 2.21 eV. (c) Top view and (d) side view of the $BNT_{(4,0)}$-8Li-24H_2 system.

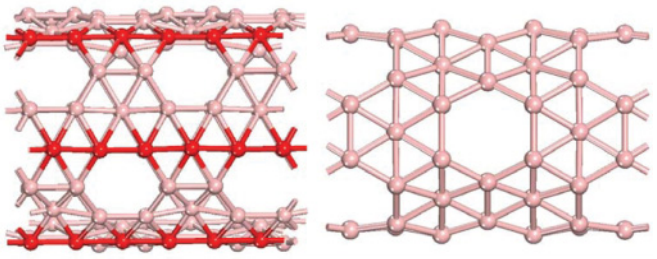

(a) (b)

FIG. 11. (Color online) (a) Side view of the (3,3) BNT and (b) side view of the (4,0) BNT. The red atoms in (a) will become the arris formed by two faces when the tube is deformed into a hexagonal one.

shows that H *s* orbitals overlap with the B 2*p* orbitals at about −6.56 eV (−6.64 eV). The *s*-*p* hybridization also strengthens the adsorption of H_C (H_D) to the B substrate.[40]

E. BNTs with different diameters or chiralities

It is important to know if the results reported above for (2,2) BNT hold for other nanotubes and how they depend on the diameter and chirality. Therefore we have also studied Li-coated (3,3) and (4,0) nanotubes.

We first consider the coating of Li onto a zigzag (3,3) BNT. As shown in Fig. 9(a), this tube is deformed into a hexagonal one, which agrees well with the case of Ca-coated (3,3) BNT.[23] Here the first two attached H_2 molecules are also adsorbed by each Li atom strongly with the adsorption energies (E_{ad}) of 0.16–0.18 eV/H_2 [Fig. 9(b)], whereas the third H_2 molecules attached to each Li move toward the corners [Fig. 9(c)]. The calculated adsorption energy (E_{ad}) for the $BNT_{(3,3)}$-12Li-36H_2 system can reach up to 0.12 eV/H_2, indicating that the corners also have the capacity to adsorb the H_2 molecules. Hence, we put 12 more H_2 molecules in the spare room around the corners and the calculated adsorption energy (E_{ad}) for the optimized $BNT_{(3,3)}$-12Li-48H_2 system [Figs. 9(d) and 9(e)] is 0.10 eV/H_2. It is evident that the radial deformation in this nanotube can also leads to a enhancement of hydrogen uptake, and thus, the final hydrogen gravimetric density can reach up to 7.94 wt%. Then, we turn to investigate the coating of Li onto a armchair (4,0) BNT. As shown in Figs. 10(a) and 10(b), no obvious radial deformation can be observed when multiple Li atoms are bound. As a result, only three H_2 molecules can be adsorbed around each Li atom [Figs. 10(c) and 10(d)] with the ideal adsorption energies (E_{ad}) of 0.12–0.18 eV/H_2 and the final hydrogen gravimetric density is merely 6.08 wt%.

The difference between the zigzag (3,3) BNT and the armchair (4,0) BNT comes from their different structural characteristics. As shown in Fig. 11(a), the red atoms in a straight line will become the arris formed by two faces when the tube is deformed into a hexagonal one, which merely distort some B-B-B bonds. However, if the atoms in a straight line parallel to the central axis of the (4,0) BNT become such an arris [Fig. 11(b)], some boron triangular lattices would be broken, suggesting that the radial deformation can hardly take place in the armchair BNTs. Furthermore, the radial deformation might be found in other Li-coated (*n*,*n*) BNT, which would be deformed into a 2*n*-polygonal one. Nonetheless, the radial deformation induced enhancement of hydrogen uptake is not suitable for all the zigzag (*n*,*n*) BNTs. Here the adsorption energy E_{ad} of H_2 molecules onto the corners of the (2,2) BNT (namely, 0.12–0.13 eV/H_2) is slightly higher than those of the (3,3) BNT (namely, 0.10–0.12 eV/H_2). On the one hand, the curvature at each corner of the (3,3) BNT becomes smaller, thus the capacity of the corners adsorbing the H_2 molecules will decrease.[38] On the other hand, the spare room around each corner has been reduced gradually [Figs. 2(a) and 9(a)] and the repulsion from the previously adsorbed H_2 molecules will also limit the uptake of the additional H_2 molecules. Therefore, as the diameter of the zigzag BNTs increases, the H_2 molecules are mainly adsorbed by the Li atoms.[29]

IV. CONCLUSION

In summary, we have used density functional theory calculations to show that Li-coated (2,2) BNT exhibits high hydrogen storage capacity (∼7.94 wt%). The hydrogen adsorption energy of 0.12–0.20 eV/H_2 (at the GGA level) suggests that desorption of hydrogen near room temperature is very likely. The H_2 molecules can be adsorbed not only on the Li atoms, but also on the BNT. The polarization interaction and orbitals hybridization are responsible for the binding of hydrogen to Li-coated BNT system. On the experimental side, the single-walled boron nanotubes were successfully synthesized,[26] which has provided a way to realize Li-coated BNT proposed here. We anticipate that the theoretical results here will also provide a useful reference for searching effective hydrogen storage materials in the laboratory.

ACKNOWLEDGMENTS

This work was supported by the National Science Foundation of China under Grant No. 10774148, the special Funds for Major State Basic Research Project of China (973) under Grant No. 2007CB925004, and the Knowledge Innovation Program of the Chinese Academy of Sciences Grants No. KJCX2-YW-W07 and No. KJCX2-YW-N35. Parts of the calculations were performed at the Center for Computational Science of CASHIPS.

*csliu@theory.issp.ac.cn.
†zzeng@theory.issp.ac.cn.

[1] See the special issue *Toward a Hydrogen Economy*, by R. Coontz and B. Hanson, Science **305**, 957 (2004).
[2] T. Yildirim and S. Ciraci, Phys. Rev. Lett. **94**, 175501 (2005).
[3] W. Liu, Y. H. Zhao, Y. Li, Q. Jiang, and E. J. Lavernia, J. Phys. Chem. C **113**, 2028 (2009).

[4]Q. Sun, Q. Wang, P. Jena, and Y. Kawazoe, J. AM. Chem. Soc. **127**, 14582 (2005).
[5]Q. Sun, P. Jena, Q. Wang, and M. Marquez, J. AM. Chem. Soc. **128**, 9741 (2006).
[6]Y. F. Zhao, Y. H. Kim, A. C. Dillon, M. J. Heben, and S. B. Zhang, Phys. Rev. Lett. **94**, 155504 (2005).
[7]M. Yoon, S. Y. Yang, C. Hicke, E. G. Wang, D. Geohegan, and Z. Y. Zhang, Phys. Rev. Lett. **100**, 206806 (2008).
[8]Q. Peng, G. Chen, H. Mizuseki, and Y. Kawazoe, J. Chem. Phys. **131**, 214505 (2009).
[9]E. Durgun, S. Ciraci, W. Zhou, and T. Yildirim, Phys. Rev. Lett. **97**, 226102 (2006).
[10]W. Zhou, T. Yildirim, E. Durgun, and S. Ciraci, Phys. Rev. B **76**, 085434 (2007).
[11]C. S. Liu and Z. Zeng, Phys. Rev. B **79**, 245419 (2009).
[12]G. Kim, S. H. Jhi, N. Park, S. G. Louie, and M. L. Cohen, Phys. Rev. B **78**, 085408 (2008).
[13]C. Ataca, E. Aktürk, and S. Ciraci, Phys. Rev. B **79**, 041406 (2009).
[14]C. S. Liu and Z. Zeng, Appl. Phys. Lett. **96**, 123106 (2010).
[15]Z. M. Ao and F. M. Peeters, Phys. Rev. B **81**, 205406 (2010).
[16]G. J. Kubas, J. Organoment. Chem. **635**, 37 (2001).
[17]G. J. Kubas, Proc. Natl. Acad. Sci. USA **104**, 6901 (2007).
[18]M. Yoon, S. Y. Yang, E. G. Wang, and Z. Y. Zhang, Nano Lett. **7**, 2578 (2007).
[19]S. Meng, E. Kaxiras, and Z. Y. Zhang, Nano Lett. **7**, 663 (2007).
[20]J. Zhou, Q. Wang, Q. Sun, P. Jena, and X. S. Chen, Proc. Natl. Acad. Sci. USA **107**, 2801 (2010).
[21]Q. Sun, Q. Wang, and P. Jena, Appl. Phys. Lett. **94**, 013111 (2009).
[22]Y. C. Li, G. Zhou, J. Li, B. L. Gu, and W. H. Duan, J. Phys. Chem. C **112**, 19268 (2008).
[23]M. Li, Y. F. Li, Z. Zhou, P. W. Shen, and Z. F. Chen, Nano Lett. **9**, 1944 (2009).
[24]H. Tang and S. Ismail-Beigi, Phys. Rev. Lett. **99**, 115501 (2007).
[25]N. Gonzalez Szwacki, A. Sadrzadeh, and B. I. Yakobson, Phys. Rev. Lett. **98**, 166804 (2007).
[26]D. Ciuparu, R. F. Klie, Y. Zhu, and L. Pfefferle, J. Phys. Chem. B **108**, 3967 (2004).
[27]X. B. Yang, Y. Ding, and J. Ni, Phys. Rev. B **77**, 041402(R) (2008).
[28]A. K. Singh, A. Sadrzadeh, and B. I. Yakobson, Nano Lett. **8**, 1314 (2008).
[29]S. Er, G. A. de Wijs, and G. Brocks, J. Phys. Chem. C **113**, 18962 (2009).
[30]Z. Zhou, J. Zhao, X. Gao, Z. Chen, J. Yan, P. v. R. Schleyer, and M. Morinaga, Chem. Mater. **17**, 992 (2005).
[31]W. Kohn and L. J. Sham, Phys. Rev. **140**, A1133 (1965).
[32]M. Schluter and L. J. Sham, Phys. Today **35**(2), 36 (1982).
[33]Y. Wang and J. P. Perdew, Phys. Rev. B **44**, 13298 (1991).
[34]H. Jósson, G. Mills, and K. W. Jacobsen, in *Nudged Elastic Band Method for Finding Minimum Energy Paths of Transitions*. *In Classical and Quantum Dynamics in Condensed Phase Simulations*, edited by B. J. Berne, G. Ciccotti, and D. F. Coker (World Scientific, Singapore, 1998), p. 385.
[35]G. Henkelman and H. Jósson, J. Chem. Phys. **113**, 9978 (2000).
[36]D. Sheppard, R. Terrell, and G. Henkelman, J. Chem. Phys. **128**, 134106 (2008).
[37]B. K. Rao and P. Jena, Europhys. Lett. **20**, 307 (1992).
[38]M. K. Kostov, H. Cheng, A. C. Cooper, and G. P. Pez, Phys. Rev. Lett. **89**, 146105 (2002).
[39]Y. H. Kim, Y. F. Zhao, A. Williamson, M. J. Heben, and S. B. Zhang, Phys. Rev. Lett. **96**, 016102 (2006).
[40]M. Khazaei, M. S. Bahramy, N. S. Venkataramanan, H. Mizuseki, and Y. Kawazoe, J. App. Phys. **106**, 094303 (2009).